HHS Public Access

Author manuscript

Nat Med. Author manuscript; available in PMC 2016 April 01.

Published in final edited form as:

Nat Med. 2015 October ; 21(10): 1209–1215. doi:10.1038/nm.3931.

CD47 Blockade Triggers T cell-mediated Destruction of Immunogenic Tumors

Xiaojuan Liu[1,5], **Yang Pu**[2], **Kyle Cron**[2], **Liufu Deng**[2], **Justin Kline**[3], **William A. Frazier**[4], **Hairong Xu**[1], **Hua Peng**[1], **Yang-Xin Fu**[1,2,6], and **Meng Michelle Xu**[1,2,6]

[1]Institute of Biophysics and the University of Chicago jointed Group for Immunotherapy, Chinese Academy of Science Key Laboratory for Infection and Immunity, Institute of Biophysics, Chinese Academy of Sciences, China

[2]Department of Pathology and Committee on Immunology, University of Chicago, Chicago, Illinois, USA

[3]Department of Medicine and Committee on Immunology, University of Chicago, Chicago, Illinois, USA

[4]Department of Biochemistry and Molecular Biophysics, Washington University, St. Louis, USA

Abstract

Macrophage phagocytosis of tumor cells mediated by CD47-specific blocking antibodies has been proposed to be the major effector mechanism in xenograft models. Using syngeneic immunocompetent tumor models, we reveal that in the therapeutic effects of CD47 blockade depend on dendritic cell (DC) but not macrophage cross-priming of T cell responses in immunocompetent mice. The therapeutic effects of anti-CD47 antibody therapy were abrogated in T cell-deficient mice. In addition, the anti-tumor effects of CD47 blockade required expression of the cytosolic DNA sensor STING, but neither MyD88 nor TRIF, in $CD11c^+$ cells, suggesting that cytosolic sensing of DNA from tumor cells is enhanced by anti-CD47 treatment, further bridging the innate and adaptive responses. Notably, the timing of administration of standard chemotherapy markedly impacted the induction of anti-tumor T cell responses by CD47 blockade. Together, our findings indicate that CD47 blockade drives T cell-mediated elimination of immunogenic tumors.

Correspondence should be addressed to Y-X.F, yfu@uchicago.edu.
[5]Those authors contribute equally to this work
[6]These authors jointly supervised this work.

Author contribution

X.L., Y.P.,H.X., M.M.X., performed experiments. L.D, J.K., W.F., H.P., provided reagents. X.L., M.M.X, Y.X.F designed and organized experiments. K.C., J.K., and H.P. edited the manuscript. X.L., M.M.X. and Y.X.F wrote the paper. Y.X.F. guided and corresponded the work.

Competing interesting statement

All authors except W.A.F. (founder and stockholder of Vasculox, Inc., St. Louis, MO) declare that they have no competing financial interests.

INTRODUCTION

Phagocytosis relies on a balance between pro-phagocytic ("eat me") and anti-phagocytic ("don't eat me") signals on target cells[1–3]. CD47, initially observed on stem cells, is a transmembrane protein that inhibits phagocytosis by binding to its receptor, signal regulatory protein α (SIRPα) which is expressed on phagocytes[4–6]. Lack of CD47 on erythrocytes, platelets and lymphohematopoetic cells results in rapid clearance of these cells by macrophages, due to elimination of the CD47-SIRPα mediated don't-eat-me signal[4,5,7,8]. Binding of CD47 to SIRPα results in phosphorylation of immunoreceptor tyrosine-based inhibitory motifs (ITIMs) onSIRPα, and recruitment of Src homology phosphatase 1 and 2 (SHP-1 and SHP-2), both of which inhibit accumulation of myosin-IIA at the phagocytic synapse[9].

Abundant CD47 expression has been also observed on a variety of malignant cells including both hematopoietic and solid tumors, especially tumor initiating cells, where elevated CD47 expression has predicted poor survival in cancer patients[10–14]. These data provide a strong rationale for therapeutic targeting of CD47[12,15]. Human CD47-blocking monoclonal antibodies (mAbs) have demonstrated efficacy in various preclinical models of human lymphoma, bladder cancer, colon cancer, glioblastoma, breast cancer ALL and AML[11,12,16–18]. Most work concluded the therapeutic effects were macrophage-dependent. However, these studies employed xenografted human tumors in T cell deficient mice[16,18,19]. Thus, it was not able to evaluate the role of adaptive immunity in the effectiveness of CD47 blockade. A previous study showed that knockdown of CD47 on tumors with morpholino in WT mice enhanced the tumoricidal activity of $CD8^+$ T cells when combined with irradiation[20]. But irradiation alone is known to stimulate anti-tumor $CD8^+$ T cell response[21]. Therefore, it remains unclear how CD47 knockdown and antibody blockade alone controls tumor growth in an immunocompetent host harboring a syngeneic tumor.

Here, we show that the therapeutic effect of CD47 blockade in syngeneic tumor models largely depends on the activation of T cells. More specifically, we demonstrate that the therapeutic effects of anti-CD47 relies on a cytosolic DNA sensor, dendritic cells (DCs), type I/II IFNs, and CD8 T cells. As such, we conclude that anti-CD47-mediated tumor rejection requires both innate and adaptive immune responses.

RESULTS

T cells are essential for anti-CD47-mediated tumor regression

To evaluate whether treatment with an anti-mouse CD47 mAb (MIAP301), known to functionally inhibit CD47-SIRPα interactions, could reduce tumor burden in syngeneic wild-type mice, BALB/c mice were subcutaneously inoculated with the CD47-positive A20 B cell lymphoma cells. Seven days later, anti-CD47 mAb was administered intraperitoneally, and tumor growth was monitored. Compared to isotype control antibody-treated animals, systemic anti-CD47 Ab treatment slowed the growth of tumor and prolonged the survival of mice bearing immunogenic A20 tumors (Fig. 1a, Supplementary Fig.1a). To extend these findings to a solid tumor model, we similarly treated syngeneic mice bearing established MC38 tumors, and observed similar results (Supplementary Fig.

1b–c). To focus on the effect of anti-CD47 within the tumor microenvironment and rule out any effect on peripheral tissues, anti-CD47 mAb was administrated by intratumoral injection in both the A20 and MC38 models (Fig.1b–c). After only two doses of anti-CD47 mAb, established tumors completely regressed. Since anti-CD47Ab might have off-target effects[22], a high affinity Sirpα variant Fc fusion protein (SIRPα-hIg) was employed as a second approach to antagonize CD47-SIRPα interactions *in vivo*[23]. Consistently, intratumoral blockade of CD47-SIPRα interactions via this approach recapitulated the inhibition of A20 tumor growth triggered by CD47 antibody blockade (Fig.1d).

We next addressed the extent to which the anti-tumor effect of CD47 blockade depended on host T cells. Thus, A20 lymphoma cells were inoculated subcutaneously into syngenic Balb/c nude mice. The same short course of intra-tumoral anti-CD47 treatment that was efficacious in wild-type Balb/c mice had no effect on tumor growth in T cell-deficient nude mice (Fig.1e). Although a longer course of consecutive anti-CD47 mAb administration resulted in a transient suppression of tumor growth in tumor-bearing nude mice (Fig.1f), T cells were clearly required for a maximal therapeutic effect of CD47 blockade therapy.

To understand which T cell subsets were involved in anti-CD47 mediated tumor reduction, wild-type mice bearing established A20 tumors were treated with anti-CD47 mAb intra-tumorally in conjunction with $CD8^+$ or $CD4^+$ T cell depletion achieved with the intra-peritoneal delivery of anti-CD4 or anti-CD8 mAbs. In the absence of $CD8^+$ T cells, the therapeutic effect of anti-CD47 was completely abrogated, while depletion of $CD4^+$ T cells had no effect (Fig.2a). $CD8^+$ or $CD4^+$ T cells were also depleted in mice systemically treated with anti-CD47 mAb. These tumors grew faster in the absence of $CD8^+$ T cells, indicating that this T cell subset is required for tumor regression also following systemic CD47 blockade (Supplementary Fig. 2a–b).

To determine whether the immune response initiated by anti-CD47 treatment resulted in T cell-mediated memory against tumor antigens, mice that had rejected A20 lymphomas after an initial course of CD47 blockade (tumor-free > 30 days) were re-challenged with a higher dose of A20 cells (2.5×10^7 cells) in the contralateral flank. Compared to naïve mice, in which a primary A20 cell challenge resulted in rapid tumor progression, those that had rejected a initial tumor challenge after CD47 blockade were completely resistant to a re-challenge of A20 cells (Fig.2b). These results clearly demonstratethat anti-CD47 treatment can elicit durable systemic immune memory to prevent relapse.

To determine whether anti-CD47 treatment can enhance tumor antigen-specific T cell responses, mice harboring established OVA-expressing MC38 tumors were treated with anti-CD47 or isotype control antibody intra-tumorally.. Five days after CD47 blockade, cells from the tumor-draining lymph node were re-stimulated in vitro with or without the OVA-derived SIINFEKL peptide, and IFN-γ production was measured by ELISPOT. Significantly more numbers of IFN-γ spot-forming cells were present in anti-CD47-treated versus isotype control antibody-treatmed (Fig. 2c). Similar results were observed in the A20 model where irradiated A20 cells were utilized to re-stimulate tumor-draining lymph node cells in vitro (Fig. 2d). To determine whether IFN-γ was essential for the therapeutic effect of anti-CD47, we treated mice bearing A20 tumors with IFN-γ-blocking antibodies on the day of anti-

CD47 treatment. The therapeutic effect of anti-CD47 was completely lost in this experimental setting (Fig. 2e). Collectively, these data suggest that an antigen-specific T cell response is enhanced after anti-CD47 treatment for both carcinoma and lymphoma tumor types.

Anti-CD47 enhances DC cross-priming for tumor control

A recent study demonstrated that macrophages, and not DCs, were the major APCs that cross-prime $CD8^+$ T cells after CD47 blockade in an *in vitro* xeno-culture system[24]. To verify these results, an *in vitro* syngeneic culture system was utilized, in which both bone marrow derived macrophages (BMDM) and bone marrow derived DCs (BMDC) were probed for their ability to cross-prime $CD8^+$ T cells in the presence or absence of anti-CD47 mAb. While anti-CD47 did not significantly increase the cross-priming abilities of BMDMs, BMDCs were able to cross-prime $CD8^+$ T cells to a greater extent than BMDMs in general, but particularly in the presence of anti-CD47 mAb (Fig. 3a).

To evaluate the cross-priming capacity of DC and macrophages in response to anti-CD47 Ab in vivo, DCs and macrophages from either the MC38 tumor microenvironment or draining lymph nodes (DLN) of anti-CD47-treated MC38-OTI-bearing mice were collected and co-cultured with OVA-specific OT-I T cells. DCs and macrophages were isolated by FACS, and their purity was validated by quantitative RT-PCR using the lineage-defining transcription factors *mafB* (macrophages) and *Zbtb46* (DCs) (Supplementary Fig. 3a). We hypothesized that anti-CD47 would increase phagocytosis inside the tumor, leading to migration of antigen-loaded APCs to the DLN where they would fully mature and cross-prime naïve T cells. However, we did not observe significant cross priming by either macrophages or DCs from the DLN from anti-CD47 treated mice (Fig. 3b). In contrast primary DCs, but not macrophages, harvested from the tumor microenvironment, clearly elicited increased activation of T cells after anti-CD47 treatment (Fig. 3c). We observed similar effects using macrophages and DCs from mice bearing A20-HA (hemagglutinin) lymphomas after co-culture with HA-reactive T cells from CL4 T cell receptor (TCR) transgenic (Tg) mice, whichTCR is specific for the HA antigen. We observed augmented T cell cross-priming induced by DCs compared to macrophages, suggesting that anti-CD47 mAb therapy enhances the ability of DCs (but not macrophages) to cross-prime T cells across tumor subtypes (Supplementary Fig. 4a). This was also the case when parental A20 or MC38 tumors were analyzed, indicating that DC-mediated cross-priming of T cells specific for naturally-expressed tumor antigens was also enhanced following anti-CD47 antibody therapy (Fig. 3d–e). To assess whether anti-CD47 Ab had a similar impact in an orthotopic tumor model, we implanted TUBO, a oncogenic receptor neu^+ mammary tumor into mammary fat pads of *neu*-transgenic mice which were subsequently treated with anti-CD47 or isotype control mAbs. Here again, increased T cell cross-priming by DCs was observed when they were co-cultured with $CD8^+$ T cells isolated from TUBO tumor-bearing mice (Supplementary Fig. 4b). Together, these findings indicate that anti-CD47 therapy enhances cross-priming of antigen-specific T cells by tumor-resident DCs.

To determine if anti-CD47-induced DC activation was also required for tumor control, tumor-bearing CD11c–diphtheria toxin receptor (*Itgax*-DTR) bone marrow chimeric (BMC)

mice were inoculated with MC38 cells subcutaneously and treated with diphtheria toxin (DT) to deplete DCs during anti-CD47 treatment. The therapeutic effect of CD47 blockade was severely impaired following DC depletion in tumor-bearing mice (Fig. 3f). However, selective removal of tumor-associated macrophages by a CSF1-blocking mAb had no impact on the anti-tumor response following CD47 blockade (Supplementary Fig. 3b). These data strongly suggest that increased DC cross priming of CTL is crucial for the therapeutic effect of anti-CD47 treatment.

Requirement for DC responsiveness to type I IFNs for tumor control

Type I IFNs are known to increase the cross-priming capability of DCs after various antitumor therapies[25–29]. Therefore, we investigated whether type I IFNs were involved in cross-priming induced by CD47 blockade. First, mice with established MC38 tumors were treated with anti-CD47 or isotype control Abs. Subsequently, DCs, macrophages were sorted from tumor tissues and levels of type I IFN mRNA (*ifna* and *ifnb)* were determined by qPCR. DCs from mice treated with anti-CD47 expressed more IFN-α mRNA than DCs from mice treated with rat Ig isotype control. In contrast, anti-CD47 boosted *ifna* mRNA abundance in the monocyte and macrophage population by only 2-fold (Fig. 4a). Similar patterns were observed for *ifnb* mRNA (Fig. 4a).

To test whether type I IFNs were required for the anti-CD47 mAb-mediated anti-tumor effect in vivo, mice bearing MC38 or A20 tumors were treated with intra-tumoral injections of IFNAR-blocking Ab on days 0 and 2 after injection with anti-CD47 or isotype control. Blocking type I IFN signaling impaired the therapeutic effect of anti-CD47 mAb (Fig.4b, Supplementary Fig.3), suggesting that type I IFNs are essential for anti-CD47-mediated tumor regression. Given the important role of type I IFNs on DC activation and the importance of DCs in anti-CD47-mediated therapeutic effects, we assessed whether type I IFN signaling specifically in DCs was required for tumor responses following CD47 blockade. To this end, MC38 tumors were established in *Cd11c*Cre^{+-}*Ifnar1*$^{fl/fl}$ mice and *Ifnar1*$^{fl/fl}$ mice. Conditional deletion of *Ifnar1* in CD11c^{+} cells markedly reduced the effect of CD47 blockade on tumor growth (Fig. 4c), demonstrating that type I IFN signaling in DCs is necessary for the therapeutic efficacy of anti-CD47 mAb. Because CD11c is known to be expressed on cells other than DCs, a DC cross-priming assay was performed using BMDCs. The cross-priming capacity of BMDCs from *ifnar1*-deficient mice in the presence of anti-CD47 mAb was compromised compared to BMDCs from wild-type mice (Fig. 4d). Together, these data indicate that type I IFN signaling in DCs plays an integral role in boosting the adaptive immune response to anti-CD47 antibody therapy.

Essential role for cytosolic DNA sensing for cross priming

Anti-CD47-induced phagocytosis might preferentially target stressed tumor cells expressing high levels of “eat me” molecules. Substances released by tumor cells engulfed into phagosomes might also promote activation of host APCs[30–32]. For example, tumor-derived danger-associated molecular patterns (DAMPs) engulfed during phagocytosis could initiate type I IFN production by engaging TLR-MyD88 sensing pathways in host APCs[31,33]. To determine whether host TLR pathways were required for the anti-tumor effect of anti-CD47 therapy, MC38 tumors were established in *Myd88*$^{-/-}$ and *Trif*$^{-/-}$ mice. The inhibition of

tumor growth after anti-CD47 treatment was comparable in WT, *Myd88*$^{-/-}$ and *Trif*$^{-/-}$ mice (Fig. 5a,b), indicating that TLR signaling in host cells is dispensable for the anti-tumor effect of CD47 blockade. These results also strongly suggest that anti-CD47 activates cross-priming through a TLR-independent pathway.

Recent studies have revealed a cytosolic DNA-sensing pathway involving the endoplasmic reticulum-resident protein STING[34–38]. The STING pathway is also essential for host DC sensing of tumor DNA[39,40]. To determine the role of STING in anti-CD47-mediated anti-tumor responses, we implanted MC38 tumor cells in flanks of wild-type and *Tmem173*^{gt} (STING-deficient) mice and monitored tumor growth after treatment with anti-CD47 or isotype control mAbs. Tumor growth was identical in WT and in *Tmem173*^{gt} mice treated with isotype control antibody. However, the anti-tumor effects of anti-CD47 treatment were completely abrogated in *Tmem173*^{gt} mice (Fig. 5c). Thus, cytosolic DNA sensing through STING is absolutely essential for the antitumor effect of anti-CD47 therapy.

To evaluate whether STINGI was essential for induction of type I IFN after anti-CD47 therapy, WT or *Tmem173*^{gt} mice bearing MC38 tumors were treated with anti-CD47 mAb. Five days later, *ifna* mRNA expression levels were measured in tumor-infiltrating DCs. A significant induction of *ifna* transcripts was observed in DCs from wild-type, but not *Tmem173*^{gt} mice following CD47 blockade (Fig. 5d). To determine whether anti-CD47-induced DC cross-priming of CD8^{+} T cells depended on STING, a cross-priming assay was conducted with BMDCs from wild-type and *Tmem173*^{gt} mice. The cross-priming capacity of wild-type but not *Tmem173*^{gt} DCs was significantly increased by co-culture with tumor cells and anti-CD47 (Fig.5e). Similar conclusions were reached by IFN-γ ELISPOT assay of purified CD8^{+} T cells from tumor draining lymph nodes (DLNs) of wild-type and *Tmem173*^{gt} mice treated with anti-CD47 mAb; anti-CD47- induced tumor-specific CD8^{+} T cell IFN-γ production in wild-type, but not *Tmem173*^{gt} mice (Fig. 5f). Overall, these results suggest that the STING-dependent cytosolic DNA sensing pathway is essential for anti-CD47-induced anti-tumor adaptive immune responses.

Chemotherapy influences anti-CD47 effects

Clinical trials of anti-CD47 treatment are underway, but many patients might also have received or continue to receive chemotherapy. As our data reveal an essential role of T cells, and as chemotherapy can suppress the immune system and kill recently activated immune cells[41,42], chemotherapy may blunt the therapeutic effects of anti-CD47 antibody therapy. Alternatively, chemotherapy may synergize with anti-CD47 by increasing release of antigens and DNA from dying tumor cells. To test whether chemotherapy drugs used for lymphoma synergize with or inhibit anti-CD47 therapy, anti-CD47 treatment was combined with clinical equivalent doses of cyclophosphamide (CTX) or paclitaxel (PTX) to treat large, established tumors. PTX (40 mg/kg) or CTX (60 mg/kg) was administered 3 days before or after anti-CD47 treatment. Chemotherapy administered after anti-CD47 treatment did not result in faster tumor regression than anti-CD47 alone (Fig.6a, b). To test the impact of chemotherapy on anti-CD47 mediated acute and memory immune responses, all tumors were surgically removed. One week after surgery, mice were re-challenged with 1.5×10^{7} A20 cells. All mice whose primary tumor underwent anti-CD47 treatment alone rejected the

tumor re-challenge (Fig. 6c). In contrast, a majority of the mice treated with anti-CD47 followed by chemotherapy were susceptible to tumor outgrowth after re-challenge (50% of CTX combination mice; 80% of PTX combination mice) (Fig. 6c–d, Table 1). This suggests that chemotherapy administered after anti-CD47 therapy had detrimental effects on development of beneficial anti-tumor memory immune responses.

We speculated that there might be a limited window of time when chemotherapy drugs can effectively reduce tumor burden and induce “eat me” signals without destroying anti-CD47-induced immunity. To test whether chemotherapy given before anti-CD47 also inhibited immune memory, an identical dose of PTX or CTX was injected 1 day prior to antibody treatment rather than 3 days after. This single treatment of chemotherapy prior to anti-CD47 not only synergized with anti-CD47 for tumor control, but also preserved the host memory response against relapsing tumors generated by anti-CD47 (100% of CTX combination mice and 80% of PTX combination mice resistant to tumor re-challenge) (Fig. 6a–c; Table 1). Taken together, our results indicate that simple alterations to standard drug administration could have a major impact on primary and memory immune responses to tumors and alter clinical outcomes in response to immunomodulatory antibody therapy.

DISCUSSION

Previous publications suggested that anti-CD47 therapy exerts anti-tumor activity by blocking "do-not-eat-me" signaling, leading to tumor cell death by macrophage-mediated phagocytosis in a manner independent of adaptive immunity[12,16,18]. In contrast, here we reveal that in immune competent mice, the therapeutic effect of low doses of anti-CD47 largely depends on DC cross-priming of CD8 T cells. Within DCs, STING mediated sensing of DNA, which drives type I IFN production, is also required. Finally, we demonstrate that timely combination of conventional therapeutics with immunotherapy can boost the host response to control or even eradicate tumors, and prevent future relapse.

Potential reasons for the differences between our conclusions and those of previous studies include differences in the preclinical animal models used[12,16]. Most previous studies used tumor xenograft models, which are widely used as preclinical models and are an integral part of the FDA approval process. Anti-human CD47 showed impressive efficacy towards xenografted human tumor cells (especially lymphoma and leukemia) in NSG mice (NOD Scid-IL2Rgamma chain deficient mice without T and B cells)[16,18]. By comparing syngeneic mouse tumors in WT and T cell-deficient nude mice, we revealed a role for T cells in the therapeutic effects of anti-CD47. Several factors could explain the apparently strong role for phagocytosis observed in xenograft models. First, as human tumor cells are “missing self” upon implantation in a NSG to activate mouse innate cells and human CD47 could become the most important “don’t-eat-me” signal expressed and crucially prevent phagocytosis. Human CD47 binds to NOD mouse SIRPα due to a germline SIRPα mutation in NOD these mice, while human CD47 could not bind well to SIRPα in other strains of mice including Balb/c and C57BL/6[43,44]. This unique binding between human CD47 and NOD mouse SIRPα on activated innate cells makes them more susceptible to antibody blockade. Secondly, in xenograft models, the therapeutic effect of anti-human CD47 was often achieved at much higher doses (e.g., 200μg daily for consecutive 14 days) than the current

study [12]. We did observe better tumor control when higher dose of anti-mouse CD47 antibody was used even in nude model. Lastly, in a syngeneic setting anti-CD47 will bind both to healthy and malignant cells that express CD47. However in the xenograft model only tumor cells express human CD47.

Our work may differ from published works in another way: using an *in vitro* serum–free assay, a recent study showed phagocytosis of human tumor cells after anti-CD47 treatment is mainly attributed to mouse bone marrow derived macrophages (BMDM), while BMDC contribution is almost undetectable[24]. Consistently, enhancement of cross-priming by macrophages was observed in response to anti-CD47. Conversely, we observed that both BMDCs as well as primary DCs are more potent than BMDMs or primary macrophages for cross priming T cells. To explain this contradiction, we have observed that culturing BMDCs without serum results in increased apoptosis and malfunction of the DCs, which could ultimately impair their cross priming capacity (Supplementary Fig. 6). Supplemented with serum, BMDCs recovered their ability to cross prime *in vitro*. Furthermore, *ex vivo* isolated DCs have stronger ability for cross priming. Finally, deletion of DCs *in vivo* limits the anti-tumor effects of anti-CD47 mAb and the anti-tumor effect of the anti-CD47 mAb depends on IFNAR on $CD11c^+$ cells. Thus, our data clearly demonstrates in immune competent syngeneic host, the therapeutic effect of CD47 blockade requires functional DCs.

Another point related to the clinical scenario is tumor immunogenicity. Accumulating evidence suggests that the response to immunotherapies is often reliant on the immunogenicity of a tumor, with tumors bearing high loads of somatic mutations showing greater responsiveness than tumors bearing relatively few somatic mutations. Highly mutated tumors likely express higher numbers of neoantigens that can be better recognized and rejected by host T cells, for example, when the CTLA-4 or PD-1 co-inhibitory pathways are blocked by therapeutic antibodies[45,46] As such, it is possible that anti-CD47 Ab treatment could possibly have more impact on immunogenic tumors than non-immunogenic tumors.

Finally, standard chemotherapy can have major impacts on anti-CD47 therapy efficacy. Prior studies have shown that chemotherapy can lead to increased expression of cell surface calreticulin on tumor cells[42]. Thus, chemotherapy-mediated up-regulation of cell surface calreticulin, an “eat-me” signal, may potentially augment the efficacy of anti-CD47 antibodies by propagating STING signaling. In addition, chemotherapy may lead to increased infiltration of APCs, including DCs and macrophages, to tumor sites[47,48]. However, properly inducing CD8 T cell-mediated tumor regression requires careful design of sequence and doses for both chemotherapy drugs and anti-CD47 Ab, as inappropriate combination treatments of antibody plus chemotherapy may have negative effects on the host immune response to tumor antigens. Thus future clinical trials involving anti-CD47 Ab treatment and standard of care chemotherapy must be properly timed and tested as both synergy and interference will be time and dose dependent. In conclusion, understanding mechanisms by which CD47 blockade interfaces with host anti-tumor immunity will yield important mechanistic information for designing novel treatments using combinations of CD47Abs with chemotherapeutics and other immunomoduatory antibodies.

METHODS

Mice

Six- to eight-week old female C57BL/6J mice were purchased from Harlan or Jackson laboratory. Six- to eight-week old female Balb/c mice were purchased from Charles River laboratory in China. *Myd88*$^{-/-}$, *Trif*$^{-/-}$, *Tmem173*^{gt}, OT-I CD8^{+} T cell receptor (TCR)-Tg, CD11c–Cre-Tg, CD11c(*itgax*)-DTR and Balb/c-Tg (*MMTV-neu*) mice were purchased from The Jackson Laboratory. *ifnar1*$^{flox/flox}$mice were kindly provided by Dr. Ulrich Kalinke from the Institute for Experimental Infection Research, Hanover, Germany. All the mice were maintained under specific pathogen free conditions and used between 6–12 weeks of age in accordance to the animal experimental guidelines set by the Institutional Animal Care and Use Committee of the University of Chicago and Institute of Biophysics, CAS.

Cell lines and reagents

All cell lines were characterized by short tandem repeat analysis (STR) profiling and tested free of mycoplasma contamination..MC38 is a murine colon adenocarcinoma cell line. A20 is a murine B cell lymphoma cell line. MC38–OTI was sorted and subcloned after MC38 cells were stable transduced with retrovirus expressing mouse EGFRVIII–OTI. A20-HA was selected as a single clone after being transduced by retrovirus expressing hemagglutination antigen (HA). TUBO was cloned from a spontaneous mammary tumor in a BALB *neu* Tg mouse[49]. Anti-IFN-γ neutralizing mAb (clone R46A2) was provided by Dr. Zhihai Qin (the Institute of Biophysics, CAS). Anti-CSF1 neutralizing mAb (5A1) and anti–mIFNAR1 neutralizing mAb (clone MAR1–5A3) were purchased from BioXcell (West Lebanon, NH). Anti-CD47 antibody (clone MIAP301) was initially purchased from ebioscience or biolegend and then provided by Dr. William Frazier (Washington University, St Louis). It is a rat-derived antibody specific recognizes mouse CD47 and blocks mouse SIRPα binding[50]. SIRPα-hIg, anti-CD8 depleting antibody (clone TIB210) and anti-CD4 depleting antibody (clone GK1.5) were produced in house. The endotoxin level for Ab and fusion protein is lower than 0.2 EU (Endotoxin Units)/μg of protein. Chemotherapeutic agents cyclophosphamide (CTX), paclitaxel (PTX), and doxorubicin (DOX) were purchased from Sigma and prepared according to the Manufacturers' recommendations.

Tumor Growth and Treatments

2–5×10^{6} A20 or 1×10^{6} MC38 tumor cells were subcutaneously injected into the flank of mice. Tumor volumes were measured by length (a) and width (b) and calculated as tumor volume = ab^{2}/2. Tumors, allowed to grow for 7–14 days to reach 50mm^{3},were treated by anti-CD47 mAb or Rat Ig intratumorally or i.p. For Sirpα-hIg treatment, 5×10^{6} A20 tumor cells were subcutaneously injected into the flank of mice. Tumors were allowed to grow for 14 days and treated by Sirpα-hIg or human Ig intratumorally. For CD8 or CD4 depletion experiments, 200–300 μg of anti-CD8 antibody (clone TIB210) or anti-CD4 antibody (clone GK1.5) was injected i.p. at the same time as anti-CD47 antibody treatment. For the IFN-γ neutralizing experiment, 300 μg of anti-mouse IFN-γ antibody (clone R46A2) was injected i.p. on the day of anti-CD47 antibody treatment. For type I IFN blockade experiments, 50μg anti-IFNAR1 mAb was intratumorally injected on day 0 and 2 after anti-CD47 Ab. For the CSF1 neutralizing experiment, 100 μg of anti-mouse CSF1 antibody (clone 5A1) was

injected i.t. on the same day of anti-CD47 antibody treatment. For chemotherapeutic agent combination, 60 mg/kg of CTX, 40 mg/kg of PTX, or 15 mg/kg of DOX were administered i.p. at the indicated times.

Production of Sirpα-hIg fusion protein

Sirpα-hIg was generated as previously[23]. Generally speaking, a plasmid encoding the DNA sequence of Sirpa was synthesized by OriGene technology company. The DNA was then cloned into the pEE12.4 expression plasmid (Lonza, Basel, Switzerland) between the IgG IgGκ leading sequence and the human IgG1 Fc sequence using BsiWI and BstBI. The SIRPa-hIg fusion protein was transiently expressed in FreeStyle™ 293-F cells.

Generation of bone marrow chimeras

WT mice were lethally irradiated with a single dose of 1000 rads. The next day irradiated mice were adoptively transferred with 2–3×10^6 CD11c–DTR Tg donor bone marrow cells. Mice were maintained on sulfamethoxazole and trimethoprim (Bactrim) antibiotics diluted in drinking water for 5 weeks after reconstitution. Mice were injected with tumor cells 5–6 weeks post reconstitution.

In vitro culture and function assay of BMDCs and BMDMs

Single-cell suspensions of bone marrow cells were obtained from C57BL/6J, *Tmem173*^{gt} or *infar1*$^{-/-}$ mice. The cells were placed in 10 cm petri dish and cultured in RPMI-1640 medium containing 10% fetal bovine serum, supplemented with 20ng/ml GM-CSF or M-CSF. Fresh media with GM-CSF or M-CSF was added into culture on day 3. BMDCs and BMDMs were harvest for stimulation assay on day 7. BMDCs or BMDMs were added and co-cultured with MC38-OTI cells at the ratio of 1:1 in the presence of fresh GM-CSF with/out 10 μg/ml anti-CD47 Ab overnight. Subsequently purified $CD11c^+$ cells and $F4/80^+$ by FCS sorting were incubated with isolated $CD8^+$ T cells from naive OT-I mice for three days.

T cell isolation

OT-I naïve $CD8^+$ T cells were isolated from lymph nodes and spleen of 6-to 12-week-old mice. Selection was carried out with a negative CD8 isolation kit (Stemcell Technologies) following manufacture's instruction.

RNA extraction and quantitative real-time RT-PCR

Total RNA from 5×10^4 sorted tumor infiltrating monocytes, macrophages and DCs were extracted with the RNeasy Micro Kit (QIAGEN) and reversed-transcribed with Seniscript Reverse Transcription Kit (QIAGEN). Real-time RT-PCR was performed with SSoFast EvaGreen supermix (Bio-Rad) according to the manufacturer's instructions and different primer sets on StepOne Plus (Applied Biosystems). Data were normalized by the level of HPRT expression in each individual sample. $2^{-\Delta\Delta Ct}$ method was used to calculate relative expression changes.

Tumor digestion

Tumor tissues were excised on day 5 after anti-CD47 Ab and digested with 1 mg/ml Collagenase IV(Sigma), 100 mg/ml DNaseI (Sigma) in the incubator with 5% CO_2. After 30 minutes, tumors were passed through a 70 μm cell strainer to remove large pieces of undigested tumor. Tumor infiltrating cells were washed twice with PBS containing 2 mM EDTA.

Measurement of IFN-γ-Secreting $CD8^+$ T Cells by ELISPOT Assay

For bone-marrow $CD11c^+$ cells functional assay, 2×10^4 purified $CD11c^+$ or $F4/80^+$ cells with were incubated with isolated $CD8^+$ T cells from naive OT-I mice with EasySep™ Mouse CD8α Positive Selection Kit (STEMCELL) for three days at the ratio of 1:10. For tumor-specific $CD8^+$ T cells functional assay in MC38-OTI model, 5 days after anti-CD47 mAb treatment, tumor DLNs were removed and $CD8^+$ T cells were purified. 2×10^5 $CD8^+$ T cells were incubated with BMDC at the ratio of 10:1 for 48 hours with/out 5μg/ml OTI peptide (SIINFEKL). For tumor-specific $CD8^+$ T cells functional assay in MC38 and A20 models, 5 days after anti-CD47 Ab treatment, tumor DLNs were removed. DLN cells were re-stimulated with A20 or MC38. 96-well HTS-IP plate (Millipore) was pre-coated with anti-IFN-γ antibody (ebiosceince) with a 1:250 dilution overnight at 4 °C. After co-culture, cells were removed, 2 μg/ml biotinylated anti-IFN-γ antibody (ebiosceince) with a 1:250 dilution was added, and the plate was incubated for 2h at room temperature or overnight at 4 °C. Avidin-horseradish peroxidase (BD Pharmingen) with a 1:1000 dilution was then added and the plate was incubated for 1h at room temperature. The cytokine spots of IFN-γ were developed according to product protocol (Millipore).

Ex vivo DC cross-presentation assay

MC38-OTIp bearing mice were treated with 50 μg of RatIg or anti-CD47 mAb intratumoral injection on days 11 and 14. Five days later, draining lymph node and tumor were digested and DCs or macrophages were purified by FACS-sorting. Approximately 5×10^4 DCs were mixed together with purified 5×10^5 OTI T cells for three days. The supernatants were collected, and IFN-γ was measured by Flex Set CBA assay (BD Bioscience).

A20-HA bearing mice were treated with 50μg of Rat Ig or anti-CD47 mAb intratumoral injection on days 10. Four days later, draining lymph nodes were digested and DCs or macrophages were purified by FACS-sorting. Approximately 4×10^3 DCs or macrophages were mixed together with purified 2×10^4 CL4 T cells for two days. IFN-γ-producing cells were enumerated by ELISPOT assay.

For tumor endougenous antigen, A20 or MC38 or TUBO bearing mice were treated with 50 μg of RatIg or anti-CD47 Ab intratumorally. Four days later, and tumor were digested and DCs or macrophages were purified by FACS-sorting. Approximately 3×10^4 DCs were mixed together with purified 3×10^5 $CD8^+$ T cells isolated from draining lymph node of mice that had been vaccined with freeze-thawed tumor cells. After 48 hours, IFN-γ-producing cells were enumerated by ELISPOT assay.

Flow Cytometric Sorting and Analysis

Single cell suspensions were blocked with anti–FcR (clone 2.4G2, BioXcell) and then stained with antibodies against CD11c (Clone N418), CD11b (Clone M1/70), Ly6C (Clone HK1.4), Ly6G (Clone1A8), F4/80 (Clone BM8) and CD45 (Clone 30-F11), and 7–AAD. Cells were sorted on FACSAria II Cell Sorter (BD). For Mouse IFN–γ Flex Set CBA assay, IFN–γ detection in the supernatants was performed on FACSCalibur Flow Cytometer (BD). Data were analyzed with FlowJo Software (TriStar).

Primer sequences for real-time PCR

Primer sequences for quantitative real–time PCR were as follows: *infb* forward 5'–TGAACTCCACCAGCAGACA–3', *infb* reverse 5'– ACCACCATCCAGGCGTAG–3'; *infa1* forward 5'-TCCCCTGACCCAGGAAGATGCC–3', *infa1* reverse 5'–ATTGGCAGAGGAAGACAGGGCT–3'; *hprt* forward 5'–TGAAGAGCTACTGTAATGATCAGTCA–3', *hprt* reverse 5'–AGCAAGCTTGCAACCTTAACCA –3'. *mafB* forward 5'-TAGAAGACACAGCAGCAAGACT-3', *mafB* reverse 5'-GACGCACGCATCACAGAG-3'; *Zbtb46* forward 5'-TCCTTCTGAGTTCTTCTGATTGAG-3', *Zbtb46* reverse 5'-AGGTTGATGTAGGCTTGATTGT-3'.

Statistical Analysis

No statistical method was used to predetermine sample size. Mice were assigned at random to treatment groups for all mouse studies and, where possible, mixed among cages. There were no mice excluded from experiments. The investigators were blinded to group allocation during the experiment and when assessing the tumor size with calipers. Experiments were repeated two to three times. Data were analyzed using Prism 5.0 Software (GraphPad) and presented as mean values ± SEM. The P values were assessed using two–tailed unpaired Student's t test or two-way ANOVA with P values considered significant as follows: *P < 0.05;**P < 0.01 and ***P < 0.001. For tumor–free mice frequency, statistics were done with the log rank (Mantel–Cox) test.

Supplementary Material

Refer to Web version on PubMed Central for supplementary material.

Acknowledgements

We thank Drs. Robert Schreiber for providing us with anti-IFNAR antibody. This research was in part supported by U.S. National Institutes of Health grants CA141975 and C134563 to Y.X.F, the National 12.5 major project of China (No. 2012ZX10001006002004) to Y.X .F and H. P. Chinese academy of Sciences grant XDA09030303 and 2012CB910203 to Y.X. F. and a Dean's Award from Washington University to W.A.F.

REFERENCE

1. Gardai SJ, et al. Cell-surface calreticulin initiates clearance of viable or apoptotic cells through trans-activation of LRP on the phagocyte. Cell. 2005; 123:321–334. [PubMed: 16239148]

2. Chao MP, et al. Calreticulin is the dominant pro-phagocytic signal on multiple human cancers and is counterbalanced by CD47. Sci Transl Med. 2010; 2:63ra94.
3. Chao MP, Majeti R, Weissman IL. Programmed cell removal: a new obstacle in the road to developing cancer. Nat Rev Cancer. 2012; 12:58–67. [PubMed: 22158022]
4. Oldenborg PA, et al. Role of CD47 as a marker of self on red blood cells. Science. 2000; 288:2051–2054. [PubMed: 10856220]
5. Blazar BR, et al. CD47 (integrin-associated protein) engagement of dendritic cell and macrophage counterreceptors is required to prevent the clearance of donor lymphohematopoietic cells. J Exp Med. 2001; 194:541–549. [PubMed: 11514609]
6. Barclay AN, Van den Berg TK. The interaction between signal regulatory protein alpha (SIRPalpha) and CD47: structure, function, and therapeutic target. Annu Rev Immunol. 2014; 32:25–50. [PubMed: 24215318]
7. Yamao T, et al. Negative regulation of platelet clearance and of the macrophage phagocytic response by the transmembrane glycoprotein SHPS-1. J Biol Chem. 2002; 277:39833–39839. [PubMed: 12167615]
8. Olsson M, Bruhns P, Frazier WA, Ravetch JV, Oldenborg PA. Platelet homeostasis is regulated by platelet expression of CD47 under normal conditions and in passive immune thrombocytopenia. Blood. 2005; 105:3577–3582. [PubMed: 15665111]
9. Tsai RK, Discher DE. Inhibition of "self" engulfment through deactivation of myosin-II at the phagocytic synapse between human cells. J Cell Biol. 2008; 180:989–1003. [PubMed: 18332220]
10. Poels LG, et al. Monoclonal antibody against human ovarian tumor-associated antigens. J Natl Cancer Inst. 1986; 76:781–791. [PubMed: 3517452]
11. Jaiswal S, et al. CD47 is upregulated on circulating hematopoietic stem cells and leukemia cells to avoid phagocytosis. Cell. 2009; 138:271–285. [PubMed: 19632178]
12. Majeti R, et al. CD47 is an adverse prognostic factor and therapeutic antibody target on human acute myeloid leukemia stem cells. Cell. 2009; 138:286–299. [PubMed: 19632179]
13. Rendtlew Danielsen JM, Knudsen LM, Dahl IM, Lodahl M, Rasmussen T. Dysregulation of CD47 and the ligands thrombospondin 1 and 2 in multiple myeloma. Br J Haematol. 2007; 138:756–760. [PubMed: 17760807]
14. Chan KS, et al. Identification, molecular characterization, clinical prognosis, and therapeutic targeting of human bladder tumor-initiating cells. Proc Natl Acad Sci U S A. 2009; 106:14016–14021. [PubMed: 19666525]
15. Chan KS, Volkmer JP, Weissman I. Cancer stem cells in bladder cancer: a revisited and evolving concept. Curr Opin Urol. 2010; 20:393–397. [PubMed: 20657288]
16. Chao MP, et al. Anti-CD47 antibody synergizes with rituximab to promote phagocytosis and eradicate non-Hodgkin lymphoma. Cell. 2010; 142:699–713. [PubMed: 20813259]
17. Willingham SB, et al. The CD47-signal regulatory protein alpha (SIRPa) interaction is a therapeutic target for human solid tumors. Proc Natl Acad Sci U S A. 2012; 109:6662–6667. [PubMed: 22451913]
18. Chao MP, et al. Therapeutic antibody targeting of CD47 eliminates human acute lymphoblastic leukemia. Cancer Res. 2011; 71:1374–1384. [PubMed: 21177380]
19. Chao MP, et al. Extranodal dissemination of non-Hodgkin lymphoma requires CD47 and is inhibited by anti-CD47 antibody therapy. Blood. 2011; 118:4890–4901. [PubMed: 21828138]
20. Soto-Pantoja DR, et al. CD47 in the tumor microenvironment limits cooperation between antitumor T-cell immunity and radiotherapy. Cancer Res. 2014; 74:6771–6783. [PubMed: 25297630]
21. Lee Y, et al. Therapeutic effects of ablative radiation on local tumor require CD8+ T cells: changing strategies for cancer treatment. Blood. 2009; 114:589–595. [PubMed: 19349616]
22. Brown EJ, Frazier WA. Integrin-associated protein (CD47) and its ligands. Trends Cell Biol. 2001; 11:130–135. [PubMed: 11306274]
23. Weiskopf K, et al. Engineered SIRPalpha variants as immunotherapeutic adjuvants to anticancer antibodies. Science. 2013; 341:88–91. [PubMed: 23722425]

24. Tseng D, et al. Anti-CD47 antibody-mediated phagocytosis of cancer by macrophages primes an effective antitumor T-cell response. Proc Natl Acad Sci U S A. 2013; 110:11103–11108. [PubMed: 23690610]
25. Burnette BC, et al. The efficacy of radiotherapy relies upon induction of type i interferon-dependent innate and adaptive immunity. Cancer Res. 2011; 71:2488–2496. [PubMed: 21300764]
26. Diamond MS, et al. Type I interferon is selectively required by dendritic cells for immune rejection of tumors. J Exp Med. 2011; 208:1989–2003. [PubMed: 21930769]
27. Fuertes MB, et al. Host type I IFN signals are required for antitumor CD8+ T cell responses through CD8{alpha}+ dendritic cells. J Exp Med. 2011; 208:2005–2016. [PubMed: 21930765]
28. Stagg J, et al. Anti-ErbB-2 mAb therapy requires type I and II interferons and synergizes with anti-PD-1 or anti-CD137 mAb therapy. Proc Natl Acad Sci U S A. 2011; 108:7142–7147. [PubMed: 21482773]
29. Yang X, et al. Targeting the tumor microenvironment with interferon-beta bridges innate and adaptive immune responses. Cancer Cell. 2014; 25:37–48. [PubMed: 24434209]
30. Chen GY, Nunez G. Sterile inflammation: sensing and reacting to damage. Nat Rev Immunol. 2010; 10:826–837. [PubMed: 21088683]
31. Desmet CJ, Ishii KJ. Nucleic acid sensing at the interface between innate and adaptive immunity in vaccination. Nat Rev Immunol. 2012; 12:479–491. [PubMed: 22728526]
32. Kono H, Rock KL. How dying cells alert the immune system to danger. Nat Rev Immunol. 2008; 8:279–289. [PubMed: 18340345]
33. O'Neill LA, Golenbock D, Bowie AG. The history of Toll-like receptors - redefining innate immunity. Nat Rev Immunol. 2013; 13:453–460. [PubMed: 23681101]
34. Ishikawa H, Barber GN. STING is an endoplasmic reticulum adaptor that facilitates innate immune signalling. Nature. 2008; 455:674–678. [PubMed: 18724357]
35. Ishikawa H, Ma Z, Barber GN. STING regulates intracellular DNA-mediated, type I interferon-dependent innate immunity. Nature. 2009; 461:788–792. [PubMed: 19776740]
36. Li XD, et al. Pivotal roles of cGAS-cGAMP signaling in antiviral defense and immune adjuvant effects. Science. 2013; 341:1390–1394. [PubMed: 23989956]
37. Sun L, Wu J, Du F, Chen X, Chen ZJ. Cyclic GMP-AMP synthase is a cytosolic DNA sensor that activates the type I interferon pathway. Science. 2013; 339:786–791. [PubMed: 23258413]
38. Wu J, et al. Cyclic GMP-AMP is an endogenous second messenger in innate immune signaling by cytosolic DNA. Science. 2013; 339:826–830. [PubMed: 23258412]
39. Woo SR, et al. STING-dependent cytosolic DNA sensing mediates innate immune recognition of immunogenic tumors. Immunity. 2014; 41:830–842. [PubMed: 25517615]
40. Deng L, et al. STING-Dependent Cytosolic DNA Sensing Promotes Radiation-Induced Type I Interferon-Dependent Antitumor Immunity in Immunogenic Tumors. Immunity. 2014; 41:843–852. [PubMed: 25517616]
41. Obeid M, et al. Ecto-calreticulin in immunogenic chemotherapy. Immunol Rev. 2007; 220:22–34. [PubMed: 17979837]
42. Obeid M, et al. Calreticulin exposure dictates the immunogenicity of cancer cell death. Nat Med. 2007; 13:54–61. [PubMed: 17187072]
43. Takenaka K, et al. Polymorphism in Sirpa modulates engraftment of human hematopoietic stem cells. Nat Immunol. 2007; 8:1313–1323. [PubMed: 17982459]
44. Yamauchi T, et al. Polymorphic Sirpa is the genetic determinant for NOD-based mouse lines to achieve efficient human cell engraftment. Blood. 2013; 121:1316–1325. [PubMed: 23293079]
45. Matsushita H, et al. Cancer exome analysis reveals a T-cell-dependent mechanism of cancer immunoediting. Nature. 2012; 482:400–404. [PubMed: 22318521]
46. Snyder A, et al. Genetic basis for clinical response to CTLA-4 blockade in melanoma. N Engl J Med. 2014; 371:2189–2199. [PubMed: 25409260]
47. Ma Y, et al. Anticancer chemotherapy-induced intratumoral recruitment and differentiation of antigen-presenting cells. Immunity. 2013; 38:729–741. [PubMed: 23562161]
48. Ma Y, et al. CCL2/CCR2-dependent recruitment of functional antigen-presenting cells into tumors upon chemotherapy. Cancer Res. 2014; 74:436–445. [PubMed: 24302580]

49. Rovero S, et al. DNA vaccination against rat her-2/Neu p185 more effectively inhibits carcinogenesis than transplantable carcinomas in transgenic BALB/c mice. J Immunol. 2000; 165:5133–5142. [PubMed: 11046045]

50. Oldenborg PA, Gresham HD, Lindberg FP. CD47-signal regulatory protein alpha (SIRPalpha) regulates Fcgamma and complement receptor-mediated phagocytosis. J Exp Med. 2001; 193:855–862. [PubMed: 11283158]

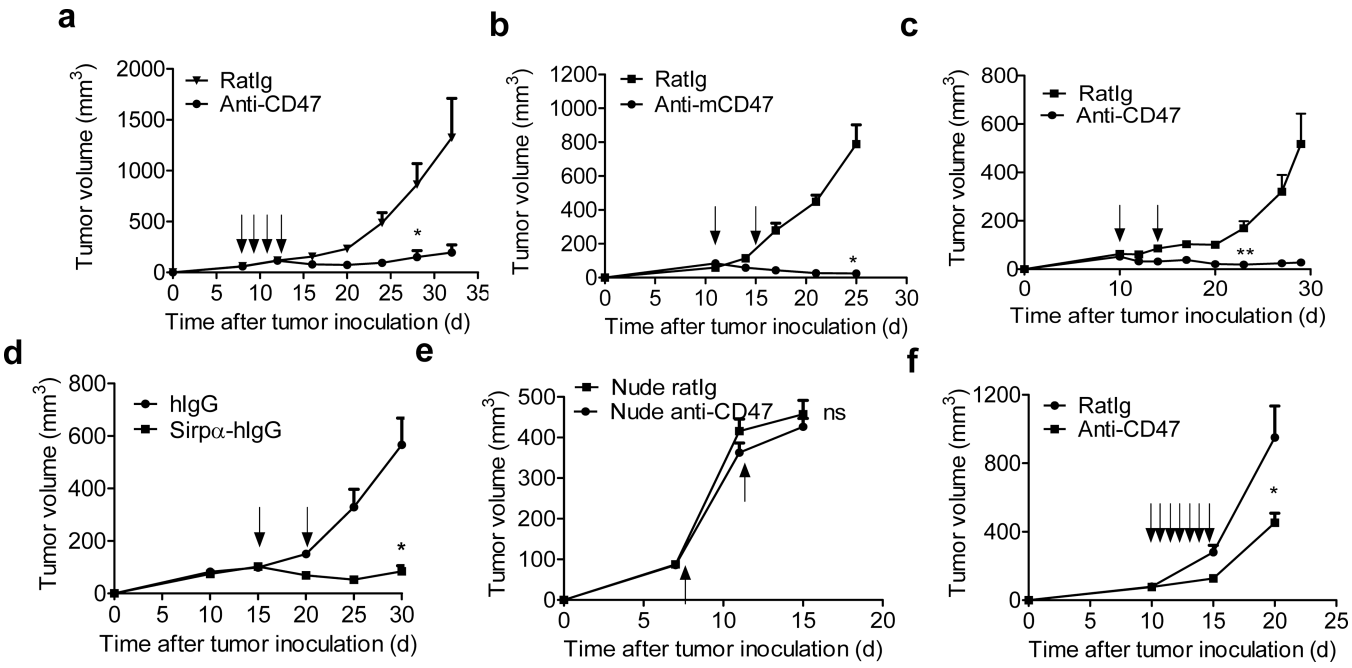

Figure 1. Anti-tumor effects of anti-CD47 depend on T cells

(a) Balb/c mice (n=5/group) transplanted s.c. with 5×10^6 A20 cells were treated intraperitoneally with 400μg of anti-mCD47or isotype control rat Ig on days 7, 9, 11 and 13. **(b)** BALB/c mice (n=5/group) were injected s.c. with 5×10^6 A20 cells and treated intratumorally with 50μg of anti-CD47 or isotype control rat Ig on days 11 and 16. **(c)** C57BL/6 mice (n=5/group) were injected s.c. with 10^6 MC38 cells and treated intratumorally with 50μg of anti-CD47 or isotype control rat Ig on days 10 and 14. One of three representative experiments is shown. **(d)** A20 tumor-bearing Balb/c mice (n=5/group) were injected s.c. with 5×10^6 A20 cells and treated twice with 50μg of Sirpα-hIg or human intratumorally on days 15 and 20 **(e)** Balb/c nude mice (n=4/group) were injected s.c. with 2×10^6 A20 cells and intratumorally injected with 50μg of anti-CD47 or isotype control rat Ig on days 7 and 11. **(f)** 2×10^6 A20 were transplanted subcutaneously on Balb/c nude mice. When tumors were established (> 50 mm^3), treatment began with daily intratumoral injections of 50 μg anti-CD47or 50 μg rat Ig for one week since day 10. Tumor growth is reported as the mean tumor size ±s.e.m. over time. One representative experiment out of three (b–c) or two (a, d-f) yielding similar results is depicted. ns (nonsignificant), *$p < 0.05$, **$P < 0.01$ (unpaired Student's t test) compared to tumors treated with RatIg.

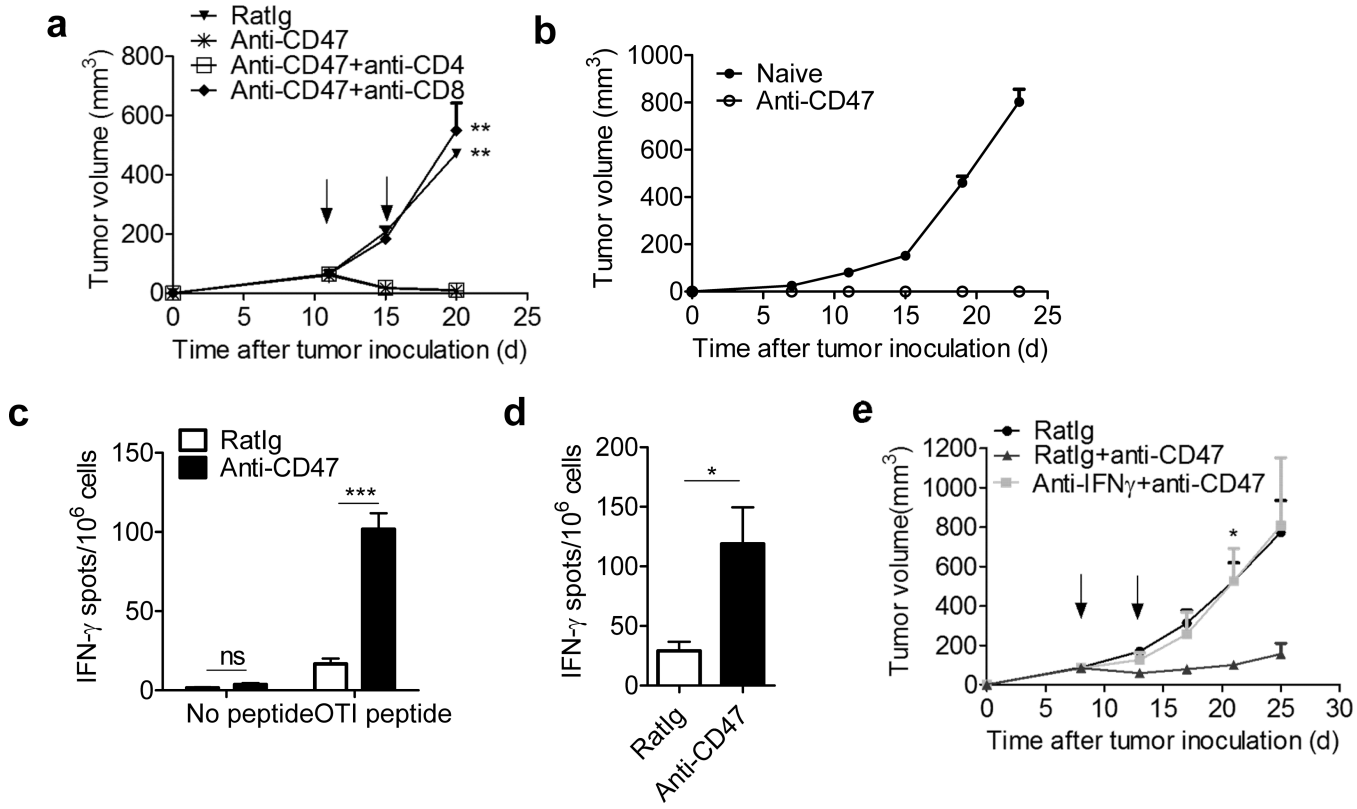

Figure 2. Therapeutic effect of anti-CD47 requires CD8$^+$ T cells

(a) BALB/c (n=8/group) mice were injected s.c. with 5×10^6 A20 and treated intratumorally with 50μg of anti-CD47 or rat Ig on days 11 and 15. 200 μg of CD8 or CD4-depleting antibody was administered twice a week, starting on day 11. **(b)** Tumor-free, antibody-treated Balb/c mice (n=7/group) were rechallenged s.c. with 2.5×10^7 A20 cells on opposite site from primary tumor one month after complete rejection. **(c)** MC38-OTI tumor bearing (n=6/group) B6 mice were i.t. treated twice with 50μg of either anti-CD47 or rat Ig on days 11 and 14. After 5 days, lymphocytes from draining LNs were isolated and stimulated with 10μg/ml OTI peptide. IFN-γ producing cells were enumerated by ELISPOT assay. **(d)** Balb/c mice (n=3) were injected s.c. with 5×10^6 A20 and i.t. treated with 50 μg of either anti-CD47 or rat Ig antibody on days 11 and 16. 7 days after the final treatment, 2×10^5 DLN cells from mice treated with anti-CD47 or rat Ig were stimulated with A20 tumor cells irradiated with 60Gy. The ratio of DLN cells to irradiated tumor was 5:1. IFN-γ -producing cells were enumerated by ELISPOT assay. **(e)** A20 tumor-bearing mice (n=5/group) were treated twice with 50μg of anti-mCD47 or rat Ig intratumorally on days 8 and 13. 300μg anti-IFNγ or rat Ig isotype control were injected intraperitoneally every four days. Data are reported as the means ±s.e.m. over time. *p < 0.05 **p < 0.01 ***p < 0.001 (unpaired Student's t test). One of three independent experiments is shown.

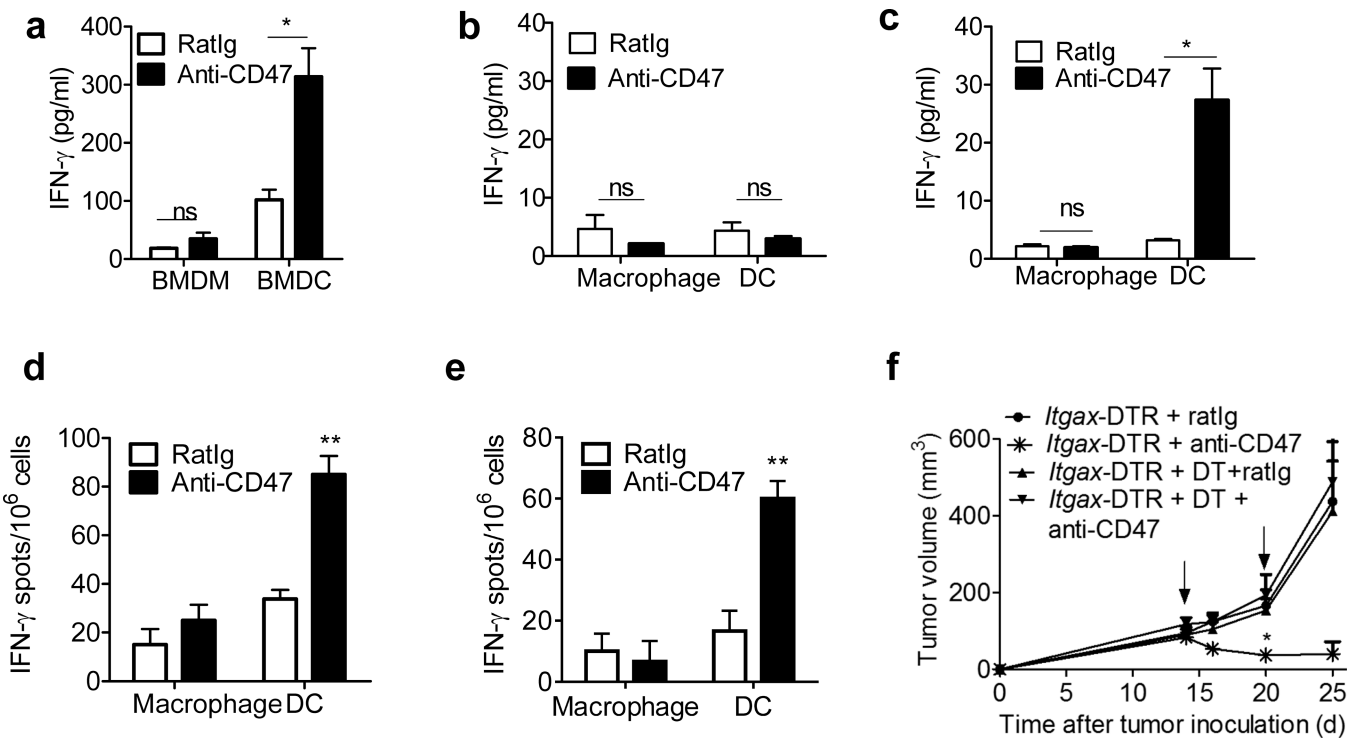

Fig3. Anti-CD47 triggers the cross-priming ability of DCs

(a) BMDCs or BMM were cultured with MC38-OTIp in the presence of fresh GM-CSF and anti-CD47 overnight. Subsequently purified $CD11c^+$ cells or $F4/80^+$ cells were co-cultured with isolated $CD8^+$ T cells from naive OTI mice for three days and analyzed by IFN-γ CBA. **(b)–(c)** MC38-OT1p bearing mice (n=5/group) were treated twice with 50μg of either anti-CD47 or rat Ig on days 11 and 14 intratumorally. Five days after the initial treatment, DLN (b) and Tumor (c) infiltrating DCs and macrophages were isolated and co-cultured with isolated $CD8^+$ T cells from naive OTI mice for three days. IFN-γ production was detected by CBA. **(d)** A20 or **(e)** MC38 tumor bearing B6 mice (n=5/group) were treated with 50 μg of either anti-CD47 or rat Ig isotype control on day 10. Four days after the antibody treatment, 3×10^4 Tumor infiltrating DCs and macrophages were isolated and co-cultured with isolated 3×10^5 $CD8^+$ T cells from A20 (d) or MC38 (e) vaccined-mice. 48 hours later, IFN-γ-producing cells were enumerated by ELISPOT assay. **(f)** 5 weeks after the indicated CD11c–DTR bone marrow chimera reconstitution, B6 mice (n=5/group) were injected subcutaneously with 10^6 MC38 cells and treated with 50μg of anti-CD47 or rat Ig on days 14 and 20. Diphtheria toxin or PBS was administrated on the same day as treatment. Data are reported as the means ±s.e.m.. *p < 0.05 **p < 0.01 ***p < 0.001 (unpaired Student's t test). One representative experiment out of three independent experiments is depicted.

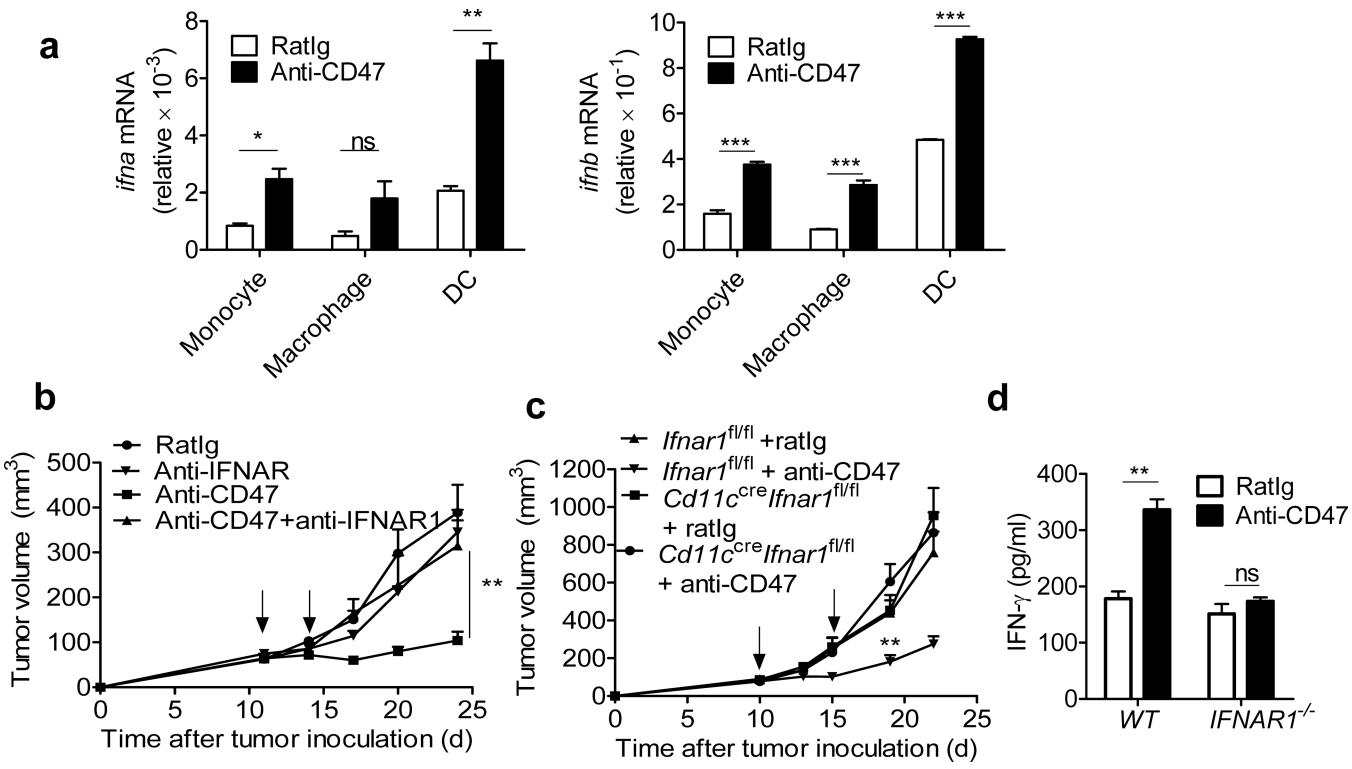

Figure4. Type I IFNs are induced during anti-CD47 mediated tumor Inhibition and required

(a) Four days after anti-CD47 or Rat Ig treatment (n=5/group), the single cell suspensions from tumors were sorted into $CD45^+CD11c\ CD11b^+Ly6c^{hi}$(Monocytes), $CD45^+CD11c^{-/+}$ $CD11b^+Ly6c\ F4/80^+$(Macrophage) and $CD45^+CD11c^+CD11b^{-/+}Ly6C\ F4/80$ (DC)populations. mRNA level of *ifna* and *ifnb* in different cell subsets were quantified by real-time PCR assay. Representative data are reported as mean copy numbers ±s.e.m. after intrasample normalization to the levels of reference gene *hprt* in three independent experiments. *p < 0.05, **p<0.01, ***p < 0.001 (unpaired Student's t test). **(b)** C57BL/6 mice (n = 6) were injected s.c. with 10^6 MC38 cells and treated intratumorally with 50μg of anti-CD47 or isotype control rat Ig on days 11 and 14. 50μg anti-IFNAR1 antibody was administered intratumorally on days 0 and 2 after anti-CD47 treatment. **(c)***Ifnar1*$^{flox/flox}$ and CD11c–Cre*Ifnar1*$^{flox/flox}$ mice (n = 6) were injected s.c. with 10^6 MC38 cells and treated with 50μg of anti-CD47 or rat Ig on days 10 and 15. **(d)** BMDCs from WT mice or *ifnar1*$^{-/-}$ mice were cultured with MC38-OTIp in the presence of anti-CD47 or rat Ig for 16h. Subsequently purified $CD11c^+$ cells were cocultured with isolated $CD8^+$ T cells from naive OT-I mice for 3 days. IFN-γ production in supernatant was determined by CBA. Data are reported as means ±s.e.m. Tumor growth is reported as the mean tumor size ±s.e.m. over time. **p < 0.01; One representative experiment out of three independent experiments is depicted.

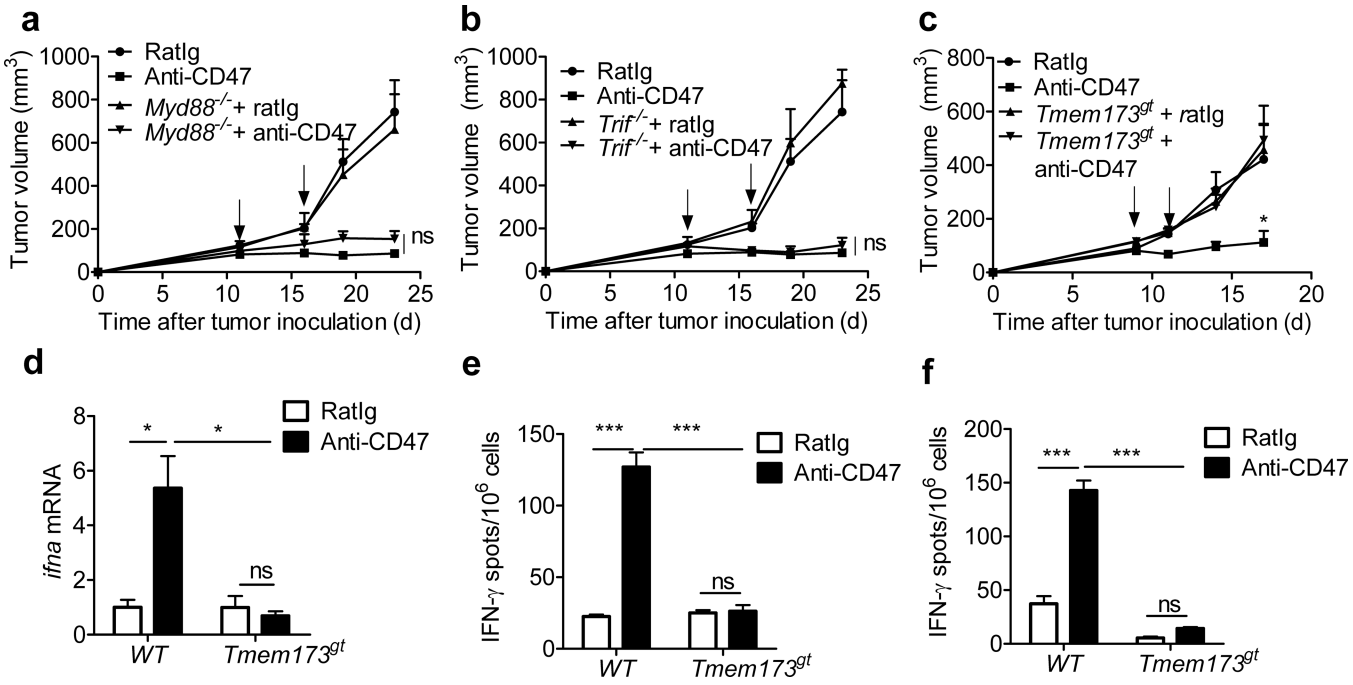

Figure5. STING signaling is required for anti-CD47 mediated tumor inhibition

MC38 tumors established (> 50mm^3) in mice were treated i.t. with anti-CD47 or rat Ig. **(a)** Tumor growth in WT and *Myd88*$^{-/-}$ mice (n=5/group) **(b)** Tumor growth in WT and *Trif*$^{-/-}$ mice (n=5/group) **(c)** Tumor growth in WT and *Tmem173*^{gt} mice (n=6/group) **(d)** WT mice or *Tmem173*^{gt} mice (n=5/group) were injected s.c. with MC38 cells and i.t. treated with 50μg of anti-CD47 on days 12 and 15. Five days after the initial treatment, DCs were sorted from tumors. mRNA level of *ifna* were quantified by real-time PCR assay. Representative data are reported as mean copy numbers ±s.e.m. after intrasample normalization to the levels of *hprt* in three independent experiments. *p < 0.05 (unpaired Student's t test). **(e)** BMDCs from WT mice or *Tmem173*^{gt}mice were cultured with MC38-OTI in the presence of anti-CD47 or rat Ig for 16h. Subsequently purified CD11c$^+$ cells were cocultured with purifed OT-I cells for 2 days. IFN-γ production was determined by ELISPOT assay. **(f)** MC38 tumor bearing B6 mice (n=5/group) were sacrificed 7 days after the final treatment. 2.5×10^5 CD8$^+$ T cells, isolated from DLNs, were stimulated with MC38 tumor cells. The ratio of CD8$^+$ T cells to MC38 was 50:1. IFN-γ-producing cells were enumerated by ELISPOT assay. Result was expressed as number of spots per 10^6 CD8$^+$ T cells. Data are reported as means ±s.e.m. *p < 0.05; **p < 0.01; ***p < 0.001(unpaired Student's t test); One of three experiments is shown.

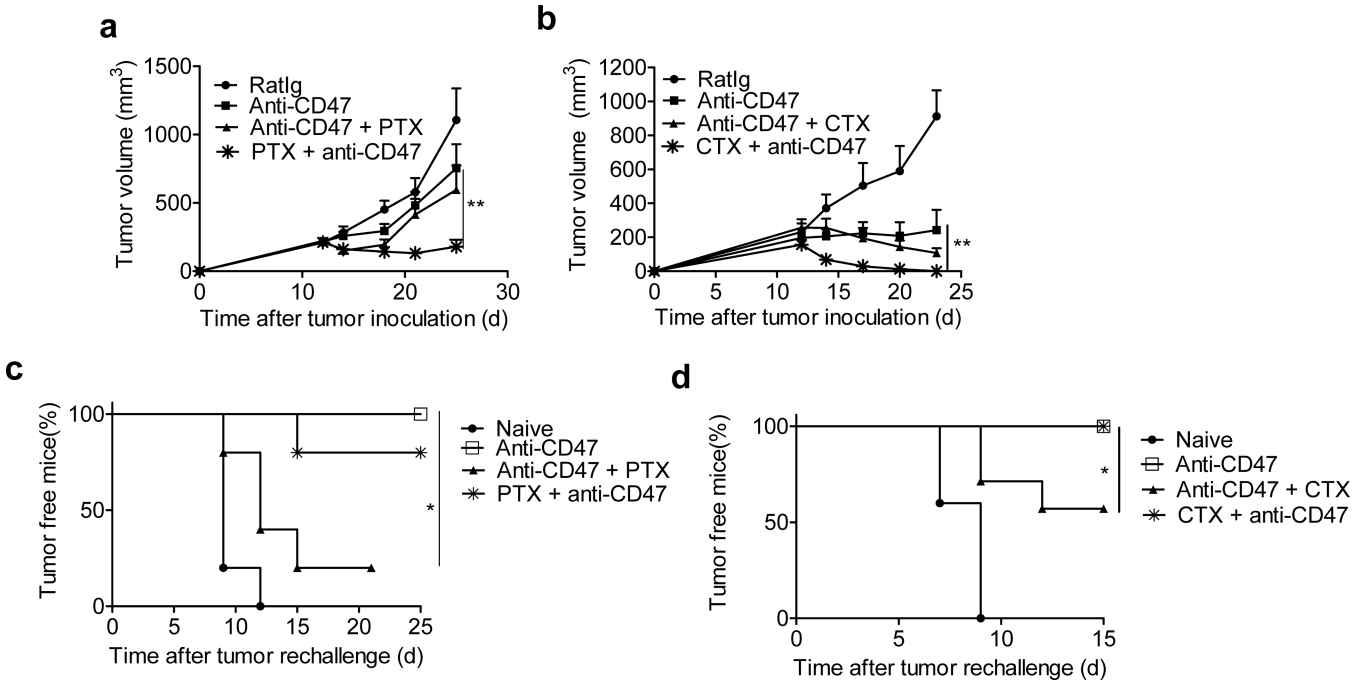

Figure 6. Anti-CD47-mediated immune protection is impaired by some post treatment Chemotherapeutics

Balb/c mice (n = 6/group) were injected s.c. with 3×10^6 A20 cells and treated with 50μg of anti-CD47 on days 12 and 17. Select chemotherapeutic agents were injected i.p. at different time points. **(a)** 40 mg/kg of PTX was injected i.p. with single dose on day 11 (one day before anti-CD47) or three doses on days 15, 18 and 21 (since 3 days post anti-CD47) (n = 7–9 pooled from two experiments). Tumor growth is reported as the mean tumor size ±s.e.m over time. **p < 0.01 (unpaired Student's t test). **(b)** 60 mg/kg of CTX (n=5/group) was injected i.p. with single dose on day 11 (one day before anti-CD47) or three doses on days 15, 18 and 21(since 3 days post anti-CD47). Tumor growth is reported as the mean tumor size ±s.e.m over time. **p < 0.01 (Two-way ANOVA). One representative experiment out of two independent experiments is depicted. **(c–d)** Treated mice (n=7/group) were removed tumors by surgery and rechallenged with 1.5×10^7 A20 cells one week after surgery. Percentage of tumor-free mice is shown. *p < 0.05 (Mantel-Cox). One representative experiment out of two independent experiments is depicted.

Table 1

Reduced memory protection after chemotherapy

	Chemotherapy			Growth After Rechallenge
Antibody dose	**Drug**	**Dosage**	**Schedule**	**Growth/Total(%)**
50 μg * 2		None		1/9 (11)
50 μg * 2	PTX	40mg/kg* 3	3 d after	4/5 (80)
50 μg * 2	PTX	40mg/kg * 1	1 d before	1/5 (20)
50 μg * 2	CTX	60mg/kg * 3	3 d after	3/6 (50)
50 μg * 2	CTX	60mg/kg * 1	1 d before	0/4 (0)